JOC The Journal of Organic Chemistry

Article

Cite This: J. Org. Chem. 2019, 84, 4050−4057

pubs.acs.org/joc

Stabilization and Extraction of Fluoride Anion Using a Tetralactam Receptor

Wenqi Liu, Allen G. Oliver, and Bradley D. Smith*

Department of Chemistry and Biochemistry, 236 Nieuwland Science Hall, University of Notre Dame, Notre Dame, Indiana 46556, United States

Supporting Information

ABSTRACT: A neutral tetralactam macrocycle was prepared in a few minutes in one pot and at high concentration using commercially available starting materials. NMR titration studies in DMSO revealed an anion affinity order of F^- > AcO^- > Cl^- > Br^-. The receptor affinity for F^- is very high due in part to formation of a self-complementary dimer comprised of two "saddle shaped" complexes. An X-ray crystal structure showed that the two F^- ions within the dimer are separated by 3.39 Å. The electrostatic penalty for this close proximity is compensated by attractive interactions provided by the surrounding tetralactam molecules. Reactivity experiments showed that stabilization of F^- as a supramolecular complex abrogated its capacity to induce elimination and substitution chemistry. This finding raises the idea of using tetralactam macrocycles to stabilize fluoride-containing liquid electrolytes within redox devices such as room-temperature fluoride-ion batteries. A lipophilic version of the tetralactam macrocycle was prepared and used to extract F^- from water into a chloroform layer with high efficiency. The favorable extraction is due to the architecture of the extracted dimeric complex, with all the polarity located within the core of the self-associated dimer and all the nonpolar functionality on the exterior surface.

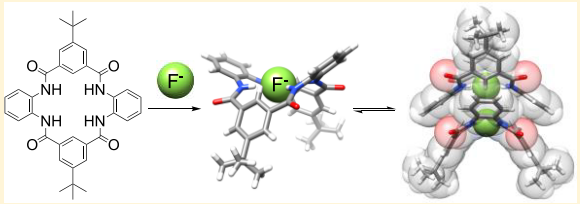

INTRODUCTION

Although anion recognition was studied early in the history of synthetic supramolecular chemistry, the early community focus was predominantly on cation recognition. But over last two decades, anion recognition has emerged as a major research subdiscipline with many potential applications in biomedicine, energy, and environmental science[1−4] One of the classic problems in anion recognition is design of synthetic receptors that selectively associate with only one of the halides. Fluoride is the smallest halide and its strong basicity and high charge-to-surface-area ratio make it a relatively easy target for selective recognition in aprotic solvents. High fluoride affinity is much harder to achieve in protic solvents where the synthetic receptors have to overcome a much higher solvation energy.[5] One way to circumvent this thermodynamic barrier is to develop synthetic receptors that incorporate Lewis acid centers such as boron, antimony or tin.[6−9] While Lewis acid receptors for fluoride have many attractive properties, they may not be the best choice in circumstances that require long-term stability or high biocompatibility. In these situations, it may be more effective to use synthetic receptors that utilize hydrogen bonding interactions via NH and OH residues.

Despite the extensive and growing literature on fluoride recognition chemistry,[10−15] very few synthetic hydrogen bonding receptors have been shown to capture or recognize fluoride in an aqueous environment.[4,16,17] In short, it is very challenging to design a hydrogen bonding system that can compete with the very high enthalpy of fluoride hydration (504 kJ mol^{-1}).[18,19] This point is highlighted by the scarcity of synthetic hydrogen bonding receptors that can extract fluoride from water.[6,7,20,21] But the need for fluoride extractors is very high since fluoride is a known pollutant that must be monitored and removed from various types of aqueous reservoirs such as polluted lakes.[22] A very different motivation to develop supramolecular receptors for fluoride is to improve the efficiency and lifetime of fluoride-containing electrolytes within redox devices such as fluoride-ion batteries which have high potential as next-generation electrochemical storage devices.[23] A key requirement for this technology is a conducting, anhydrous fluoride ion electrolyte that does not decompose through elimination chemistry.[24] An unexplored potential solution is a liquid electrolyte containing a soluble receptor that stabilizes the fluoride while still allowing high ionic conductivity. The mass scale of these two future applications (aqueous fluoride extraction and fluoride ion batteries) is enormous, and thus any practical solution based on a synthetic fluoride receptor must be cost-effective.

Our programmatic interest in supramolecular chemistry using tetralactam macrocycles[25,26] led us to consider the anion receptors reported by Jurczak and co-workers. They have systematically explored a range of tetralactams linked by flexible alkyl chains and observed anion binding in highly competitive DMSO solution.[27−30] Studies of 18-membered tetralactams were quite limited because the compounds exhibited poor solubility. One of these tetralactam receptors

Received: January 6, 2019
Published: March 4, 2019

DOI: 10.1021/acs.joc.9b00042
J. Org. Chem. 2019, 84, 4050−4057

(Scheme 1) was sufficiently soluble in DMSO for anion titration studies, and the K_a for fluoride was determined to be

Scheme 1. Jurzcak's Receptor and New Receptors 1 and 2 with Relevant Atom Labels

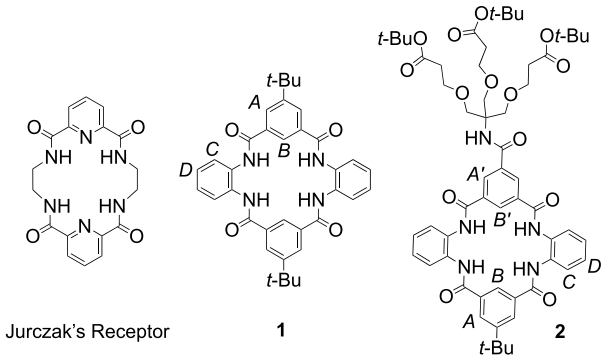

830 M^{-1}.[27] It occurred to us that tetralactam **1** might be a more soluble receptor with a highly preorganized macrocyclic structure. A literature review revealed that structural analogues of **1** have been prepared before, but they were only studied as scaffolds for copper cation binding.[31−33] Here we describe the synthesis and molecular structure of tetralactam **1** and we characterize its anion recognition ability in solution and in the solid state. We also report the analogue **2** with an appended lipophilic chain that enables extraction of fluoride from aqueous solution.

RESULTS AND DISCUSSION

Synthesis. Receptor **1** was synthesized by a simple procedure that reacted 1,2-diaminobenzene with an equal molar equivalent of 4-*tert*-butylisophthaloyl dichloride (Scheme 2). The reactions were conducted in CH_2Cl_2 using submolar concentrations of reactants and a short reaction time (10 min at room temperature), and the pure macrocycle product **1** was obtained in 26% isolated yield. During the

Scheme 2. Synthesis of 1 and 2

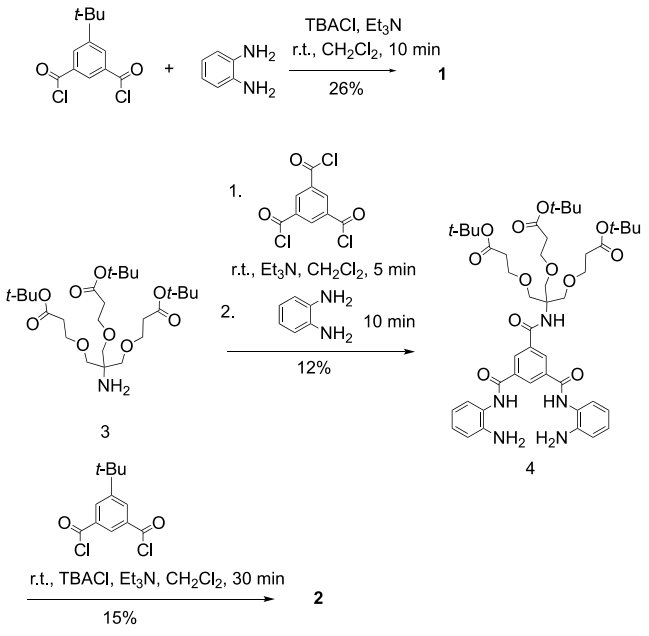

reaction optimization studies, it was found that the purification process was facilitated if tetrabutylammonium chloride ($TBA^+ \cdot Cl^-$) was included in the reaction because it formed a soluble complex with **1**. It is likely that Cl^- also promoted the desired reaction by acting as a macrocyclization template.[34] The asymmetric macrocycle **2** was prepared in two steps via intermediate Bisamine **4**. The first round of reactions provided enough material for all studies, and no attempt was made to optimize the synthetic yield. But if the synthesis was to be repeated, it is likely that the yield of the second macrocyclization step could be increased by employing literature modifications.[32]

X-ray Crystal Structures. The X-ray crystal structure of empty **1** was obtained by slow diffusion of diethyl ether into a solution of **1** dissolved in a mixture of $CHCl_3$ and DMSO at room temperature. As shown in Figure 1, the macrocycle

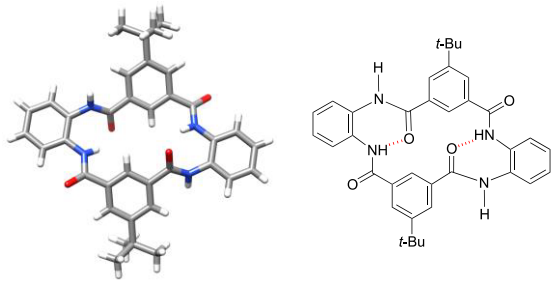

Figure 1. (Left) X-ray crystal structure of empty **1**. (Right) chemical structure highlighting the closed conformation with dashed lines indicating intramolecular hydrogen bonds. Lattice DMSO molecules are omitted for clarity.

adopts a closed conformation with two intramolecular hydrogen bonds.[28] In Figure 2 are crystal structures of **1**·Cl^-, and **1**·AcO^-, which were obtained by slow diffusion of diethyl ether into a solution of **1** and excess TBA^+ salt in $CHCl_3$/DMSO at 5 °C. In both structures, the macrocycle adopts a

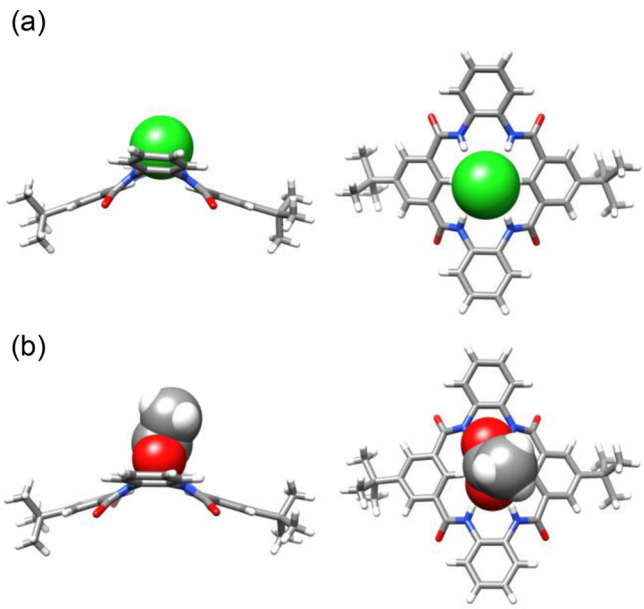

Figure 2. Side and top views of X-ray crystal structures of (a) **1**·$TBA^+ \cdot Cl^-$ and (b) **1**·$TBA^+ \cdot AcO^-$. For clarity, the TBA^+ cation is omitted in each case, so is a lattice $CHCl_3$ molecule in (b).

DOI: 10.1021/acs.joc.9b00042
J. Org. Chem. 2019, 84, 4050−4057

relatively flat conformation with the anion perched above the central cavity. Hirshfeld surface analysis[35] (Figures S8–S10) of the diffraction data indicates that the Cl^- forms hydrogen bonds with all four amide NH residues (average NH···Cl distance 2.56 Å) and the two isophthalamide CH protons (average CH···Cl distance 2.64 Å) of **1**, while the anisotropic AcO^- bridges the two pairs of amide NH residues (average NH···O distance 1.98 Å) and interacts less strongly with the two isophthalamide CH protons (average CH···O distance 2.82 Å).

A single crystal of **1**·F^- was obtained by slow diffusion of pentane into a solution of **1** and excess TBA^+·F^- in $CHCl_3$/DMSO at 5 °C. X-ray diffraction analysis of the crystal showed that the F^- is buried in the cavity and forms hydrogen bonds with all four amide NH residues (average NH···F distance 1.86 Å) and the two isophthalamide CH protons (average CH···Cl distance 2.31 Å). Unlike the relatively flat structures of **1**·TBA^+·Cl^- and **1**·TBA^+·AcO^-, the structure of **1**·TBA^+·F^- adopts a "saddle shape" with each pair of opposing aromatic rings in **1** oriented at angles of 34.24° and 54.44°. In Figure 3a is a view of the crystal for **1**·TBA^+·F^- that highlights the lattice packing as a series of homodimers, i.e., [**1**·TBA^+·F^-]$_2$, that are created by complementary head-to-head stacking of two saddle-shaped complexes. Reduced Density Gradient (RDG) analysis[36,37] (Figures S11–S12) reveals a large dimer interface for attractive π–π stacking and van der Waals interactions between the two macrocycle surfaces. These attractive interactions stabilize the repulsions caused by the dehydrated F^-···F^- distance of 3.39 Å. The two counter TBA^+ cations contact opposing exterior surfaces of the dimer and form CH···π interactions (Figure 3b). Similar CH···π interactions were also observed in the crystal structures of **1**·TBA^+·Cl and **1**·TBA^+·AcO^-.

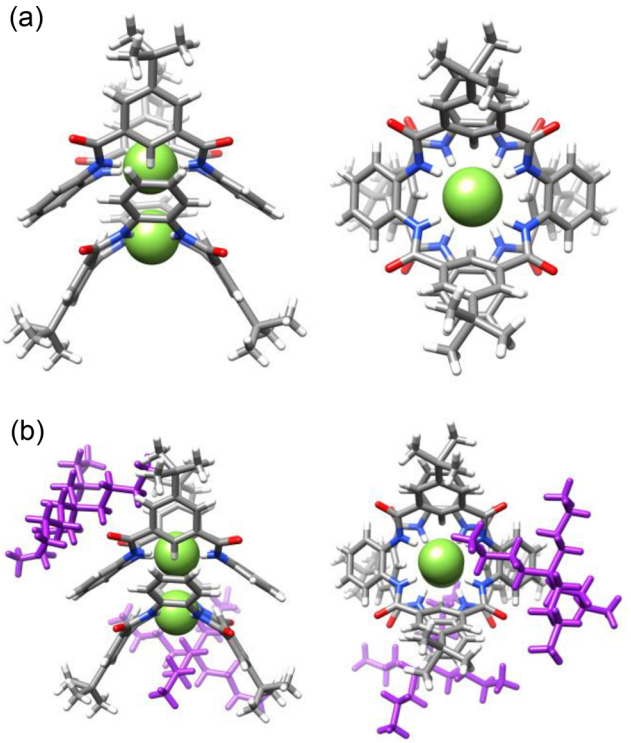

Figure 3. Side and top views of the X-ray crystal structure for **1**·TBA^+·F^-. The views in (a) highlight the self-complementary stacking of two saddle-shaped complexes to form a solid-state homodimer [**1**·F^-]$_2$, and the views in (b) show how the two TBA^+ counter cations (purple) contact the opposing exterior surfaces of the dimer. A lattice $CHCl_3$ molecule is omitted for clarity.

Solution-State Association Studies. Anion affinities for **1** were evaluated by conducting ^{1}H NMR titration experiments in DMSO-d_6 that added the anions as TBA^+ salts (Figures S13–S20). As expected, peaks for the macrocycle amide NH protons and isophthalamide protons B moved incrementally downfield as the titration progressed, indicating that anion complexation was rapid on the NMR time scale. In each case, the chemical shift for the isophthalamide protons B was plotted against anion concentration and the titration isotherms were fit to standard binding models using nonlinear computer methods. The curves for Cl^- and Br^- fitted well to a simple 1:1 binding model, whereas the isotherms for F^- or AcO^- required a binding model that formed a mixture of 1:1 and 2:1 macrocycle/anion complexes.[29,38] Listed in Table 1 are the derived associations, K_1 and K_2. As expected, the values of K_1 for the anions decreased in the order F^- > Cl^- > Br^-. It is notable that the affinity of tetralactam **1** for F^- in DMSO-d_6 is 60 times higher than Jurczak's receptor in Scheme 1,[27] five times higher than a structurally similar tetrathiolactam reported by Kanbara and Yamamoto,[39a] and 20 times higher than a related 16-membered tetralactam reported by Lin.[39b] In Figure 4 is a comparison of the ^{1}H spectra for free **1** and the spectra for **1** after adding a large molar excess of each TBA^+ salt. There is a consistent trend of higher K_1 correlating with a larger downfield change in NH chemical shift. Another distinctive feature of the NMR spectra is the difference in peaks widths. Most of the peaks for solutions of **1** saturated

Table 1. Association Constants for 1 in DMSO-d_6 at 25 °C

Guest[a]	K_1 (M^{-1})	K_2 (M^{-1})
F^-	(5.3 ± 0.8) × 10^4	(3.1 ± 0.7) × 10^3
Cl^-	(363 ± 5)	N.A.
Br^-	(23 ± 1)	N.A.
AcO^-	(1.2 ± 0.1) × 10^4	445 ± 15

[a] TBA^+ salt.

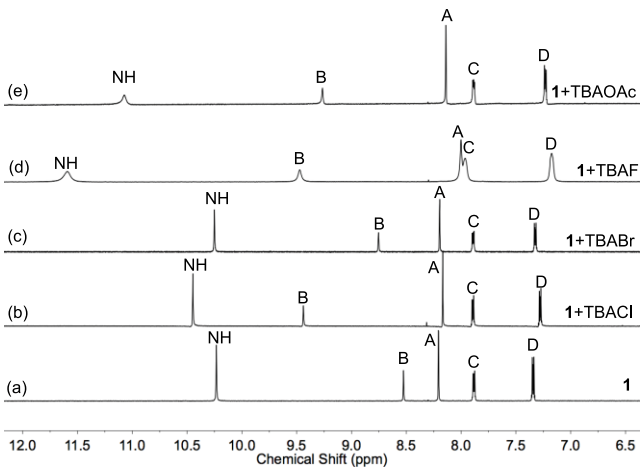

Figure 4. Partial ^{1}H NMR spectra (600 MHz, DMSO-d_6, 25 °C) of (a) free receptor **1**. Receptor **1** mixed with (b) 11 molar equiv of TBA^+·Cl^-, (c) 16 molar equiv of TBA^+·Br^-, (d) 1.8 molar equiv of TBA^+·F^-, and (e) 3.5 molar equiv of TBA^+·AcO^-.

DOI: 10.1021/acs.joc.9b00042
J. Org. Chem. 2019, 84, 4050–4057

with Cl^- or Br^- in a 1:1 stoichiometry are narrow. In comparison, most of the peaks for the solutions of **1** saturated with F^- or AcO^- are slightly broadened because the complexes are an exchanging mixture of 1:1 and 2:1 stoichiometries.

Mass spectrometric analysis (Figures 5, S1–S3) of separate chloroform samples containing **1** mixed with TBA^+ salts of F^-,

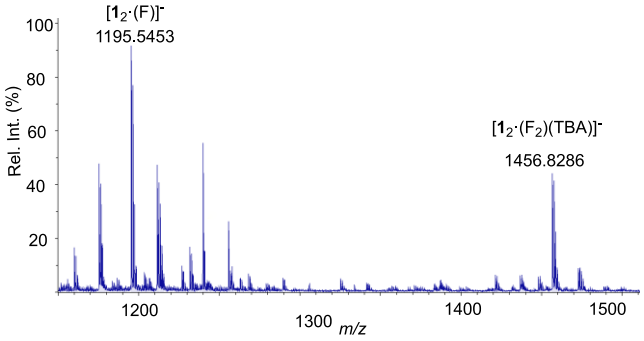

Figure 5. Negative ion HRMS (ESI) of **1**·TBA^+·F^- in $CHCl_3$.

Cl^-, Br^-, or AcO^- produced observable 1:1 complexes, and in the cases of F^- and AcO^- there were also peaks for the 2:1 complexes (i.e., [$\mathbf{1}_2$·F^-] and [$\mathbf{1}_2$·AcO^-]). Interestingly, the mass spectrum of **1** mixed with TBA·F^- also showed a strong peak for the dimeric complex [$\mathbf{1}_2$·(F^-)$_2$·TBA^+]$^-$ (Figure 5), further suggesting that the dimer is an abundant species in solution.

Computational Studies of Fluoride Association. Supramolecular complexes that contain clusters of multiple anions are rare but increasingly known.[40] In the case of complexes with multiple F^-, there are examples of single receptor molecules containing multiple F^- and also [receptor·F^-] complexes that self-associate to form aggregates.[40] Most of the F^- clusters are hydrated, but when there is no hydration, the $F^-\cdots F^-$ distance is in the range 2.91–3.26 Å.[11,41] The dehydrated $F^-\cdots F^-$ pair in dimeric [**1**·F^-]$_2$ is separated by 3.39 Å which is a comparatively long distance and suggests that the surrounding pair of macrocycles prevent closer approach and provide stability. As shown in Figure 6, a DFT energy calculation of two F^- ions separated by 3.39 Å in the gas phase produces an unfavorable binding energy of +95.5 kcal/mol. A calculated electrostatic potential map of the saddle shaped tetralactam **1** reveals a strongly positive potential at the

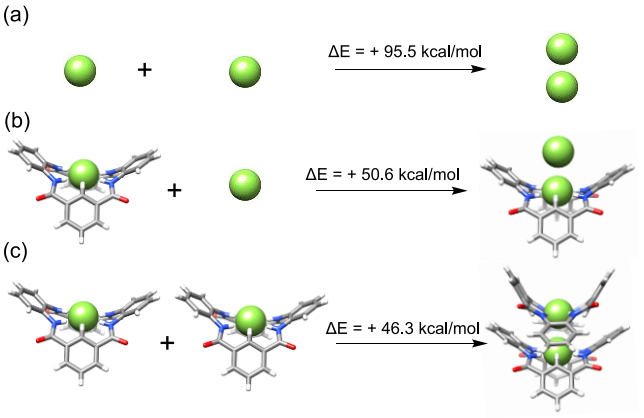

Figure 6. DFT calculation of 2 [**1**·F^-] dimerization at B3LYP-6-31G +** level.

macrocycle core (Figure S21). The binding energy is reduced to +50.6 kcal/mol when a copy of **1** is associated with one of the two separated F^- ions, and further reduced to +46.3 kcal/mol when a second copy of **1** is associated with the other F^- ion. Obviously, these binding energies would be further relieved if the counter TBA^+ cations and solvent were included in the model. Stabilization of anion dimers by a surrounding pair of cofacially stacked macrocycle receptors has been reported before for other anions such as HSO_4^-.[42]

Non-Covalent Stabilization of F^- and Attenuation of F^- Reactivity. F^- can react as a base or as a nucleophile and often induces a mixture of competing elimination and substitution chemistry.[43] Recent reports have shown how hydrogen-bonding F^- receptors can be used to favor one specific reaction pathway (usually substitution) and thus produce a desired synthetic outcome.[10,11,13] But to the best of our knowledge, a hydrogen-bonding receptor has not been shown to eliminate all F^- reactivity, a circumstance that is needed when F^- is employed as a stable electrolyte in redox devices.[23,24] We reasoned that the capability of tetralactam **1** to stabilize F^- inside self-associated dimers would lead to strong attenuation of F^- reactivity. To prove this concept, we conducted the two comparative reactions shown in Scheme 3.

Scheme 3. Effect of Tetralactam 1 on F^- Reactivity

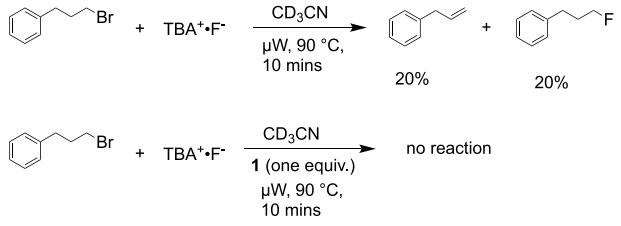

The first reaction used a microwave to heat a mixture of (3-bromopropyl)benzene and TBA$^+$·F^- in CD_3CN at 90 °C for 10 min. After heating, the reaction solution was light yellow (Figure S22), and ^{1}H NMR analysis of the solution (Figure S23) showed that 40% of the (3-bromopropyl)benzene had been converted into the expected elimination and substitution products (1:1 product ratio), along with some base promote hydrolysis and degradation of the TBA^+. The second reaction employed the same reagents and heating conditions but also included 1 molar equiv of tetralactam **1** as an additive. In this case, the solution remained colorless and ^{1}H NMR analysis (Figure S24) showed that there was no reaction. Thus, the results clearly show that tetralactams, such as **1**, have excellent ability to abrogate F^- reactivity.

Fluoride Extraction from Water. Extracting fluoride from water is important for water purification[1] and ^{18}F radiolabeling technology.[14] The modified macrocycle **2** has high solubility in common organic solvents and therefore was used for fluoride extraction experiments. First, a biphasic extraction was performed by mixing the solution of **2** (3 mM) in $CDCl_3$ (1 mL) with a solution of TBA$^+$·F^- (12 mM) in D_2O (1 mL). The extracted $CDCl_3$ layer was separated and analyzed by ^{19}F and ^{1}H NMR spectroscopy. A single ^{19}F peak was observed at 39 ppm, greatly downfield from the signal at −126 ppm for a control sample of TBA$^+$·F^- in $CDCl_3$ (Figure 7). A control extraction experiment showed that in the absence of **2** there was no ^{19}F signal in the extracted $CDCl_3$ layer. Thus, the ^{19}F NMR data indicated that tetralactam **2** extracted TBA$^+$·F^- out of water and into $CDCl_3$ by forming a complex. In Figure 8a,

DOI: 10.1021/acs.joc.9b00042
J. Org. Chem. 2019, 84, 4050–4057

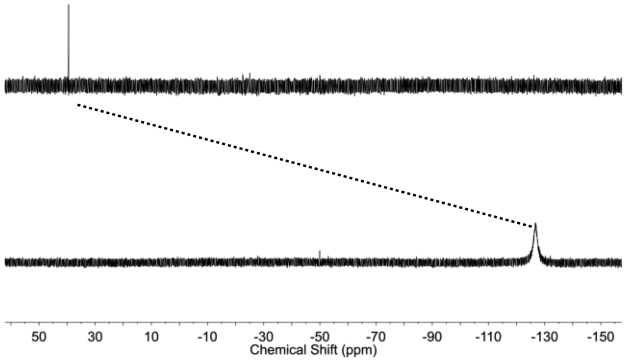

Figure 7. ^{19}F NMR (470 MHz) spectra (4-fluorobenzaldehyde as external reference) for two separate samples: (bottom) free TBA$^+$·F$^-$ in $CDCl_3$, (top) $CDCl_3$ layer containing **2**·TBA$^+$·F$^-$ after biphasic extraction experiment.

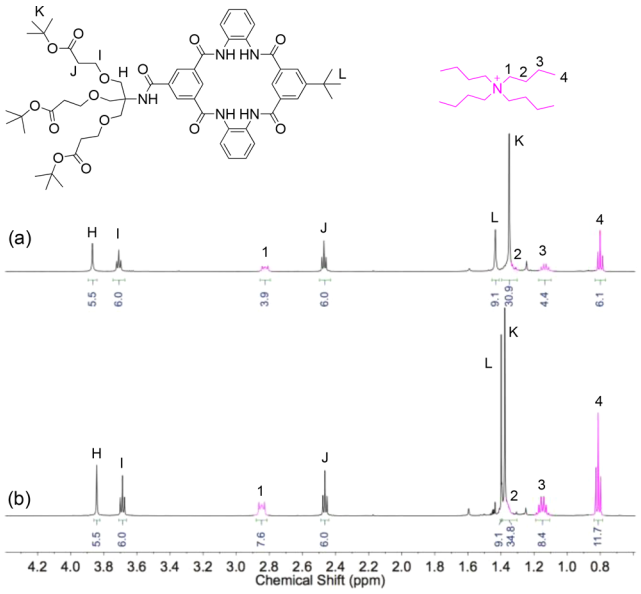

Figure 8. Partial ^{1}H NMR (500 MHz) of $CDCl_3$ layer after biphasic extraction experiment. (a) extracted complex with the formula [**2**$_2$·TBA$^+$·F$^-$], (b) extracted complex with the formula [**2**·TBA$^+$·Cl$^-$]. The complete NMR spectra and associated analysis are provided in the Supporting Information.

the ^{1}H NMR spectrum for the extracted $CDCl_3$ layer is shown. Peak integration revealed a 2:1 stoichiometry between **2** and TBA$^+$, indicating the extracted complex to have the formula [**2**$_2$·F$^-$·TBA$^+$] which is consistent with the gas phase species [**1**$_2$·F$^-$] identified by mass spectrometry in Figure 5. Furthermore, the ^{1}H NMR peaks for the TBA$^+$ cation within the extracted [**2**$_2$·F$^-$·TBA$^+$] complex were upfield of the signals for free TBA$^+$·F$^-$ in $CDCl_3$ (Figure S25) suggesting that the TBA$^+$ was associated with the exterior aromatic surface of [**2**$_2$·F$^-$]. Independent evidence for this conclusion was gained by acquiring a ^{1}H ROESY spectrum (Figure S26) of the extracted $CDCl_3$ solution and observing cross-relaxation between the TBA$^+$ protons and protons A and A′ on receptor **2** (atom labeling in Scheme 1).

The same biphasic extraction experiment was conducted using **2** and TBA$^+$·Cl$^-$. As shown by the ^{1}H NMR spectra in Figures 8b and S27, there was a 1:1 stoichiometry between **2** and TBA$^+$, indicating the extracted complex to have the formula [**2**·Cl$^-$·TBA$^+$] which is consistent with all the other data for this complex. A final experiment was a biphasic competitive extraction using **2** and an equimolar mixture of TBA$^+$·F$^-$ and TBA$^+$·Cl$^-$. Combined ^{1}H and ^{19}F NMR analyses of the extracted $CDCl_3$ layer indicated that 4% of the extracted complex contained F$^-$ and 96% contained Cl$^-$ (Figures S28–S29). This result is not surprising considering the strong Hofmeister bias for Cl$^-$ over F$^-$ due to the large difference in hydration energies. The inability to selectively extract F$^-$ over Cl$^-$ might be a limitation for environmental purification where high Cl$^-$ is a common occurrence, but this scenario is less likely to arise in ^{18}F radiolabeling technology.[14]

CONCLUSION

Macrocyclic tetralactam **1** can be prepared in one pot and high mass scale from commercially available starting materials. It has moderate solubility in organic solvents, especially when it is complexed with TBA$^+$ salts. In DMSO solution it exhibits the complexation affinity order F$^-$ > AcO$^-$ > Cl$^-$ > Br$^-$. The very high affinity for F$^-$ is noteworthy, and in DMSO solution, the **1**·F$^-$complexation stoichiometry is a mixture of 1:1 and 2:1. An X-ray crystal structure of **1**·TBA$^+$·F$^-$ reveals lattice packing of two "saddle shaped" complexes as a self-complementary dimer. The two F$^-$ ions within the dimer are separated by only 3.39 Å, and the electrostatic penalty for this close proximity is overcome by attractive interactions provided by the two surrounding receptor molecules. Because of its capability to stabilize F$^-$ inside self-associated dimers, tetralactam **1** can eliminate the propensity of F$^-$ to induce elimination and substitution chemistry. This finding raises the intriguing idea of employing tetralactam receptors, such as **1**, to stabilize fluoride-containing electrolytes within redox devices such as room-temperature fluoride-ion batteries.[23] Future investigations are needed to ascertain if tetralactams can stabilize F$^-$ in solution while still allowing rapid F$^-$ conduction and capture/release at metal fluoride electrodes.[24]

The unsymmetric tetralactam **2** with appended lipophilic groups can be prepared in two simple steps and has very high solubility in organic solvents. Biphasic extraction experiments with **2** in the organic layer and an aqueous layer containing a low millimolar concentration of TBA$^+$·F$^-$ produced saturation of **2** as a fluoride complex. The extraction efficiency is much better than most other reported examples of fluoride extraction using an uncharged hydrogen bonding receptor. Typically, 60%–80% of receptor saturation has been obtained when the starting water layer contained molar or submolar concentrations of fluoride.[6,20,21,44−46] The high extraction efficiency is due in large part to the core–shell architecture of the extracted dimeric complexes that contain one or two F$^-$ ions surrounded by two copies of self-associated **2**. All of the polar functional groups are buried within the dimer core, whereas nonpolar functionality dominates the exterior surface. If needed, the stability of the dimeric F$^-$ encapsulation process can likely be enhanced by using covalently linked versions of **2** that can act as "clam shell" receptors,[16] or alternatively **2** can be grafted onto a polymeric backbone to create an immobilized extraction agent.[20]

EXPERIMENTAL SECTION

General. ^{1}H, ^{13}C, and ^{19}F NMR spectra were recorded on a 400, 500, or 600 MHz spectrometer at 25 °C. The chemical shift is presented in ppm and referenced by a residual solvent peak. Mass spectrometry (MS) was performed using a time-of-flight spectrometer with electrospray ionization (ESI). Commercially available solvents

DOI: 10.1021/acs.joc.9b00042
J. Org. Chem. 2019, 84, 4050–4057

and chemicals were used without further purification unless otherwise stated. Water was deionized and microfiltered. Flash column chromatography was performed using silica gel as the stationary phase. 5-(*tert*-Butyl)isophthaloyl dichloride and compound **3** were synthesized according to reported procedures.[47]

Synthesis and Characterization. *Tetralactam* ***1***. 5-(*tert*-Butyl)-isophthaloyl dichloride (200 mg, 0.77 mmol) in dried CH_2Cl_2 (5 mL) was added dropwise over 2 min to a dried CH_2Cl_2 solution (5 mL) of 1,2-diaminobenzene (83 mg, 0.77 mmol), tetrabutylammonium chloride (1.1 g, 3.85 mmol), and Et_3N (0.5 mL, 3.6 mmol), and the reaction mixture was stirred at room temperature for a total of 10 min. The solvent was removed, and the residue was purified by column chromatography using 10% acetone/$CHCl_3$ to elute **1** as a white solid (60 mg, 26% yield). (Note: eluted fractions containing pure **1** gradually form a precipitate during the column chromatography process.) Mp > 260 °C. ^{1}H NMR (500 MHz, DMSO-d_6) δ 10.23 (s, 4H), 8.58−8.48 (m, 2H), 8.21 (d, J = 1.5 Hz, 4H), 7.88 (dd, J = 6.0, 3.5 Hz, 4H), 7.34 (dd, J = 6.0, 3.5 Hz, 4H), 1.38 (s, 18H). ^{13}C {^{1}H} NMR (126 MHz, DMSO-d_6) δ 165.8, 152.7, 135.2, 131.5, 128.3, 126.5, 125.8, 124.4, 35.6, 31.6. HRMS (ESI-TOF) m/z: (M + Na]$^+$ calcd for $C_{36}H_{36}N_4NaO_4^+$ 611.2629; found 611.2606.

Bis(amine) ***4***. A solution of compound **3** (1.00 g, 1.98 mmol) in dry CH_2Cl_2 (15 mL) was added dropwise over 2 min to a solution of 1,3,5-benzenetricarbonyl trichloride (0.525 g, 1.98 mmol) in dry CH_2Cl_2 (20 mL) at room temperature. Et_3N (3.8 mL,19.8 mol) was then added dropwise to the reaction, and the mixture was stirred for 5 min. Benzene-1,2-diamine (0.43g, 3.96 mmol) in dry CH_2Cl_2 was added to the reaction mixture and stirred for 10 min. The solvent was removed, and the residue was purified by column chromatography using 10% acetone in $CHCl_3$ to elute the product **4** as a yellow viscous liquid (220 mg, 12% yield). (Note: This compound was isolated with moderate purity and used for the next step without further purification.) ^{1}H NMR (600 MHz $CDCl_3$) δ 8.96 (d, J = 3.3 Hz, 2H), 8.66 (s, 1H), 8.44 (s, 2H), 7.23−7.16 (m, 2H), 7.04 (td, J = 7.7, 1.5 Hz, 2H), 6.84 (s, 1H), 6.81−6.71 (m, 4H), 3.82 (d, J = 4.6 Hz, 6H), 3.67 (t, J = 6.0 Hz, 6H), 2.44 (t, J = 6.0 Hz, 10H), 1.34 (s, 27H). ^{13}C {^{1}H} NMR (151 MHz, $CDCl_3$) δ 171.4, 166.3, 164.4, 141.4, 136.1, 134.9, 134.5, 129.9, 129.0, 127.4, 125.9, 125.8, 123.9, 119.2, 118.1, 80.8, 68.9, 67.1, 60.6, 36.4, 28.1. HRMS (ESI-TOF) m/z: (M + H]$^+$ calcd for $C_{46}H_{64}N_5O_{12}^+$ 878.4546; found 878.4565.

Macrocycle ***2***. 5-(*tert*-Butyl)isophthaloyl dichloride (64.9 mg, 0.25 mM) in dried CH_2Cl_2 (5 mL) was added over 2 min to a mixture of **4** (220 mg, 0.25 mM), TBA$^+$·Cl$^-$ (69 mg, 0.25 mM), and Et_3N (0.17 mL, 1.25 mM) in dried CH_2Cl_2 (5 mL) and stirred at room temperature for 30 min. The reaction mixture was purified by column chromatography using 10% acetone/CH_2Cl_2 to elute pure **2** as an off-white solid (41 mg, 15% yield). Mp > 260 °C. ^{1}H NMR (400 MHz, $CDCl_3$) δ 10.01 (s, 2H), 9.72 (s, 2H), 8.78−8.69 (m, 2H), 8.57 (s, 1H), 8.44−8.28 (m, 3H), 7.50 (d, J = 8.0 Hz, 4H), 6.95 (s, 1H), 6.92−6.73 (m, 4H), 3.93 (s, 6H), 3.76 (t, J = 6.0 Hz, 6H), 2.49 (t, J = 6.0 Hz, 6H), 1.54 (s, 9H), 1.33 (s, 27H). ^{13}C {^{1}H} NMR (101 MHz, $CDCl_3$) δ 171.6, 166.4, 165.8, 165.5, 153.2, 137.2, 135.4, 134.5, 131.3, 130.2, 129.8, 129.5, 128.3, 126.8, 126.1, 125.8, 123.9, 81.1, 69.4, 67.4, 60.9, 36.7, 31.6, 28.3. HRMS (ESI-TOF) m/z: (M + Na]$^+$ calcd for $C_{58}H_{73}N_5O_{14}Na^+$ 1086.5046; found 1086.5084.

General Procedure for NMR Titration. Association constants between host **1** and different guest anions were determined by standard ^{1}H NMR titration methods that added TBA$^+$ salts in DMSO-d_6 (D, 99.9%) at 25 °C. The same titration procedure was used for each replicate, and reproducibility was excellent. Standard precautions were used to exclude water, although it is likely that a small amount was absorbed by the hygroscopic solvent. The concentration of the host was between 1 mM and 3 mM. The stock solution concentration of anion guest was between 20 mM and 200 mM. The guest solution was prepared using the host solution which ensured that the concentration of host did not change over the whole titration process. Aliquots from the guest stock solution were added sequentially to an NMR tube containing **1**, and ^{1}H NMR spectrum was acquired after each addition. The chemical shift of host proton B (atom labels in Scheme 1) was fitted to a 1:1 or 2:1 association model as described further in the Supporting Information.

Molecular Modeling. The coordinates for **1** were directly extracted from the X-ray crystal structure of **1**·TBA+·F$^-$, and the *t*-Bu groups were replaced with H to reduce the calculation time. The single-point energy for each state of separated F$^-$ ions in Figure 6 was calculated by Gaussian 09 at the B3LYP/6-31+G** level without structural optimization, and frequency calculations were not performed. The binding energy is the difference between the single-point energy of the state and the sum of single-point energies for the individual components. The structures were visualized using Mercury 3.5.1.

Reactivity Experiments. A stock solution (1 mL) of (3-bromopropyl)benzene (40 mM) was prepared in CD_3CN. A stock solution (1 mL) of TBA$^+$·F$^-$·3H_2O (40 mM) was prepared in CD_3CN, and the concentration was further calibrated by ^{1}H NMR peak integration using (3-bromopropyl)benzene as an internal standard. Two reaction solutions were prepared and compared. The first solution (solution A) (1 mL) was prepared as a mixture of (3-bromopropyl)benzene (2 mM) and TBA$^+$·F$^-$ (2.7 mM). The second solution (solution B) was prepared as a mixture of (3-bromopropyl)-benzene (2 mM), TBA$^+$·F$^-$ (2.7 mM) and **1** (2.7 mM) (note that **1** is only soluble in CD_3CN when TBA$^+$·F$^-$ is present). Both solutions were heated in sealed vessels at 90 °C for 10 min using a microwave reactor. ^{1}H NMR spectra were acquired after the reaction, and the product yields were determined by peak integration.

General Procedure for Anion Extraction. A solution of **2** (3 mM, 1 mL) in $CDCl_3$ was mixed with the solution of TBA$^+$·F$^-$ (12 mM, 1 mL) in D_2O, and the solution was vortexed for 3 min. The mixture was allowed to sit for 1 h to ensure clean separation of the layers. The organic layer was separated and analyzed by ^{1}H and ^{19}F NMR. The same procedure was used for TBA$^+$·Cl$^-$ (12 mM, 1 mL) extraction, and also for the biphasic competitive extraction of TBA$^+$·F$^-$ (12 mM, 1 mL) and TBA$^+$·Cl$^-$ (12 mM, 1 mL) with **2**.

■ ASSOCIATED CONTENT

Supporting Information

The Supporting Information is available free of charge on the ACS Publications website at DOI: 10.1021/acs.joc.9b00042.

NMR spectra, mass spectra, X-ray crystallography data, Hirshfeld surface analysis, RDG calculation, computational data, NMR titration data, fluoride reactivity, and fluoride extraction data (PDF)

Crystallographic data for **1**·TBA$^+$·ACO$^-$ (CIF)

Crystallographic data for **1**·TBA$^+$·Cl$^-$ (CIF)

Crystallographic data for **1**·TBA$^+$·F$^-$ (CIF)

Crystallographic data for **1** (CIF)

■ AUTHOR INFORMATION

Corresponding Author

*E-mail: smith.115@nd.edu.

ORCID

Wenqi Liu: 0000-0001-6408-0204

Bradley D. Smith: 0000-0003-4120-3210

Notes

The authors declare no competing financial interest.

■ ACKNOWLEDGMENTS

This work was supported by a grant from the NSF (CHE1708240).

■ REFERENCES

(1) Busschaert, N.; Caltagirone, C.; Van Rossom, W.; Gale, P. A. Applications of Supramolecular Anion Recognition. *Chem. Rev.* **2015**, *115*, 8038−8155.

DOI: 10.1021/acs.joc.9b00042
J. Org. Chem. 2019, 84, 4050−4057

(2) Kang, S. O.; Begum, R. A.; Bowman-James, K. Amide-Based Ligands for Anion Coordination. *Angew. Chem., Int. Ed.* **2006**, *45*, 7882−7894.
(3) Qiao, B.; Leverick, G. M.; Zhao, W.; Flood, A. H.; Johnson, J. A.; Shao-Horn, Y. Supramolecular Regulation of Anions Enhances Conductivity and Transference Number of Lithium in Liquid Electrolytes. *J. Am. Chem. Soc.* **2018**, *140*, 10932−10936.
(4) Langton, M. J.; Serpell, C. J.; Beer, P. D. Anion Recognition in Water: Recent Advances from a Supramolecular and Macromolecular Perspective. *Angew. Chem., Int. Ed.* **2016**, *55*, 1974−1987.
(5) Cremer, P. S.; Flood, A. H.; Gibb, B. C.; Mobley, D. L. Collaborative Routes to Clarifying The Murky Waters of Aqueous Supramolecular Chemistry. *Nat. Chem.* **2017**, *10*, 8−16.
(6) Chiu, C. W.; Gabbaï, F. P. Fluoride Ion Capture from Water with a Cationic Borane. *J. Am. Chem. Soc.* **2006**, *128*, 14248−14249.
(7) Hirai, M.; Gabbaï, F. P. Squeezing Fluoride out of Water with a Neutral Bidentate Antimony(V) Lewis Acid. *Angew. Chem., Int. Ed.* **2015**, *54*, 1205−1209.
(8) Kim, Y.; Gabbaï, P. Cationic Boranes for the Complexation of Fluoride Ions in Water below the 4 ppm Maximum Contaminant Level. *J. Am. Chem. Soc.* **2009**, *131*, 3363−3369.
(9) Kuate, A. C. T.; Naseer, M. M.; Jurkschat, K. Liquid membrane transport of potassium fluoride by the organotin-based ditopic host Ph_2FSnCH_2SnFPh-CH_2-[19]-crown-6. *Chem. Commun.* **2017**, *53*, 2013−2015.
(10) Pupo, G.; Ibba, F.; Ascough, D. M. H.; Vicini, A. C.; Ricci, P.; Christensen, K. E.; Pfeifer, L.; Morphy, J. R.; Brown, J. M.; Paton, R. S.; Gouverneur, V. Asymmetric Nucleophilic Fluorination under Hydrogen Bonding Phase-Transfer Catalysis. *Science* **2018**, *360*, 638−642.
(11) Pfeifer, L.; Engle, K. M.; Pidgeon, G. W.; Sparkes, H. A.; Thompson, A. L.; Brown, J. M.; Gouverneur, V. Hydrogen-Bonded Homoleptic Fluoride−Diarylurea Complexes: Structure, Reactivity, and Coordinating Power. *J. Am. Chem. Soc.* **2016**, *138*, 13314−13325.
(12) Devi, K.; Sarma, R. J. Naphthalimide-Containing Isomeric Urea Derivatives: Mechanoluminescence and Fluoride Recognition. *ChemPhotoChem.* **2017**, *1*, 524−531.
(13) Liang, S.; Hammond, G. B.; Xu, B. Hydrogen Bonding: Regulator for Nucleophilic Fluorination. *Chem. - Eur. J.* **2017**, *23*, 17850−17861.
(14) Bowen, L. H.; Rood, T. R. Solvent Extraction of ^{18}F as Tetraphenylstibonium Fluoride. *J. Inorg. Nucl. Chem.* **1966**, *28*, 1985−1990.
(15) Clarke, H. J.; Howe, E. N. W.; Wu, X.; Sommer, F.; Yano, M.; Light, M. E.; Kubik, S.; Gale, P. A. J. Transmembrane Fluoride Transport: Direct Measurement and Selectivity Studies. *J. Am. Chem. Soc.* **2016**, *138*, 16515−16522.
(16) Kubik, S. Anion Recognition in Water. *Chem. Soc. Rev.* **2010**, *39*, 3648−3663.
(17) Ren, A.; Rajashankar, K. R.; Patel, D. J. Fluoride Ion Encapsulation by Mg^{2+} Ions and Phosphates in a Fluoride Riboswitch. *Nature* **2012**, *486*, 85−89.
(18) Cametti, M.; Rissanen, K. Recognition and Sensing of Fluoride Anion. *Chem. Commun.* **2009**, 2809−2829.
(19) Cametti, M.; Rissanen, K. Highlights on Contemporary Recognition and Sensing of Fluoride Anion in Solution and in The Solid State. *Chem. Soc. Rev.* **2013**, *42*, 2016−2038.
(20) Aydogan, A.; Coady, D. J.; Kim, S. K.; Akar, A.; Bielawski, C. W.; Marquez, M.; Sessler, J. L. Poly(methyl methacrylate)s with Pendant Calixpyrroles and Crown Ethers: Polymeric Extractants for Potassium Halides. *Angew. Chem., Int. Ed.* **2008**, *47*, 9648−9652.
(21) Ravikumar, I.; Saha, S.; Ghosh, P. Dual-Host Approach for Liquid−Liquid Extraction of Potassium Fluoride/Chloride *via* Formation of an Integrated 1-D Polymeric Complex. *Chem. Commun.* **2011**, *47*, 4721−4723.
(22) Zuo, H.; Chen, L.; Kong, M.; Qiu, L.; Lü, P.; Wu, P.; Yang, Y.; Chen, K. Toxic Effects of Fluoride on Organisms. *Life Sci.* **2018**, *198*, 18−24.
(23) Gschwind, F.; Rodriguez-garcia, G.; Sandbeck, D. J. S.; Gross, A.; Weil, M. Fluoride Ion Batteries: Theoretical Performance, Safety, Toxicity, and A Combinatorial Screening of New Electrodes. *J. Fluorine Chem.* **2016**, *182*, 76−90.
(24) Davis, V. K.; Bates, C. M.; Omichi, K.; Savoie, B. M.; Momčilović, N.; Xu, Q.; Wolf, W. J.; Webb, M. A.; Billings, K. J.; Chou, N. H.; Alayoglu, S.; McKenney, R. K.; Darolles, I. M.; Nair, N. G.; Hightower, A.; Rosenberg, D.; Ahmed, M.; Brooks, C. J.; Miller, T. F.; Grubbs, R. H.; Jones, S. C. Room-Temperature Cycling of Metal Fluoride Electrodes: Liquid Electrolytes For High-Energy Fluoride Ion Cells. *Science* **2018**, *362*, 1144−1148.
(25) Gassensmith, J. J.; Arunkumar, E.; Barr, L.; Baumes, J. M.; DiVittorio, K. M.; Johnson, J. R.; Noll, B. C.; Smith, B. D. Self-Assembly of Fluorescent Inclusion Complexes in Competitive Media Including The Interior of Living Cells. *J. Am. Chem. Soc.* **2007**, *129*, 15054−15059.
(26) Liu, W.; Johnson, A.; Smith, B. D. Guest Back-Folding: A Molecular Design Strategy That Produces a Deep-Red Fluorescent Host/Guest Pair with Picomolar Affinity in Water. *J. Am. Chem. Soc.* **2018**, *140*, 3361−3370.
(27) Szumna, A.; Jurczak, J. A New Macrocyclic Polylactam-Type Neutral Receptor for Anions − Structural Aspects of Anion Recognition. *Eur. J. Org. Chem.* **2001**, *2001*, 4031−4039.
(28) Chmielewski, M. J.; Jurczak, J. Anion Binding Versus Intramolecular Hydrogen Bonding in Neutral Macrocyclic Amides. *Chem. - Eur. J.* **2006**, *12*, 7652−7667.
(29) Chmielewski, M. J.; Jurczak, J. Anion Recognition by Neutral Macrocyclic Amides. *Chem. - Eur. J.* **2005**, *11*, 6080−6094.
(30) Chmielewski, M. J.; Zieliński, T.; Jurczak. Synthesis, Structure, and Complexing Properties of Macrocyclic Receptors for Anions. *Pure Appl. Chem.* **2007**, *79*, 1087−1096.
(31) Mo, Z.; Yang, W.; Gao, J.; Chen, H.; Kang, J. Synthesis of Three New Macrocyclic Tetraamide Ligands. *Synth. Commun.* **1999**, *29*, 2147−2153.
(32) Vandromme, L.; Monchaud, D.; Teulade-Fichou, M. P. Beneficial Effect of Mukaiyama Reagent on Macrobislactamization Reactions. *Synlett* **2006**, *2006* (20), 3423−3426.
(33) Halvagar, M. R.; Solntsev, P. V.; Lim, H.; Hedman, B.; Hodgson, K. O.; Solomon, E. I.; Cramer, C. J.; Tolman, W. B. Hydroxo-Bridged Dicopper(II,III) and -(III,III) Complexes: Models for Putative Intermediates in Oxidation Catalysis. *J. Am. Chem. Soc.* **2014**, *136*, 7269−7272.
(34) (a) Martí-Centelles, V.; Burguete, M. I.; Luis, S. V. Macrocycle Synthesis by Chloride-Templated Amide Bond Formation. *J. Org. Chem.* **2016**, *81*, 2143−2147. (b) Lichosyt, D.; Wasilek, S.; Dydio, P.; Jurczak, J. The Influence of Binding Site Geometry on Anion-Binding Selectivity: A Case Study of Macrocyclic Receptors Built on the Azulene Skeleton. *Chem. - Eur. J.* **2018**, *24*, 11683−11692. (c) Łęczycka-Wilk, K.; Dąbrowa, K.; Cmoch, P.; Jarosz, S. Chloride-Templated Macrocyclization and Anion-Binding Properties of C2-Symmetric Macrocyclic Ureas from Sucrose. *Org. Lett.* **2017**, *19*, 4596−4599. (d) Satake, A.; Ishizawa, Y.; Katagiri, H.; Kondo, S. Chloride Selective Macrocyclic Bisurea Derivatives with 2,2′-Binaphthalene Moieties as Spacers. *J. Org. Chem.* **2016**, *81*, 9848−9857. (e) Dabrowa, K.; Niedbala, P.; Majdecki, M.; Duszewski, P.; Jurczak, J. A General Method for Synthesis of Unclosed Cryptands via H-Bond Templated Macrocyclization and Subsequent Mild Post-functionalization. *Org. Lett.* **2015**, *17*, 4774−4777.
(35) Spackman, M. A.; Jayatilaka, D. Hirshfeld Surface Analysis. *CrystEngComm* **2009**, *11*, 19−32.
(36) Lu, T.; Chen, F. Multiwfn: A Multifunctional Wavefunction Analyzer. *J. Comput. Chem.* **2012**, *33*, 580−592.
(37) Johnson, E. R.; Keinan, S.; Mori Sánchez, P.; Contreras García, J.; Cohen, A. J.; Yang, W. Revealing Noncovalent Interactions. *J. Am. Chem. Soc.* **2010**, *132*, 6498−6506.
(38) Goursaud, M.; De Bernardin, P.; Cort, D.; Bartik, K.; Bruylants, G. Monitoring Fluoride Binding in DMSO: Why is a Singular Binding Behavior Observed? *Eur. J. Org. Chem.* **2012**, *2012* (19), 3570−3574.

DOI: 10.1021/acs.joc.9b00042
J. Org. Chem. 2019, 84, 4050−4057

(39) (a) Inoue, Y.; Kanbara, T.; Yamamoto, T. Preparation of A New Receptor for Anions, Macrocyclic Polythiolactam—Structure and High Anion-Binding Ability. *Tetrahedron Lett.* **2003**, *44*, 5167−5169. (b) Shang, X.; Lin, H.; Cai, Z.; Lin, H. Anion Recognition Properties of The Neutral Receptors Bearing Amide Macrocycle. *J. Heterocycl. Chem.* **2008**, *45*, 1329−1332.
(40) He, Q.; Tu, P.; Sessler, J. L. Supramolecular Chemistry of Anionic Dimers, Trimers, Tetramers, and Clusters. *Chem.* **2018**, *4*, 46−93.
(41) Curiel, D.; Cowley, A.; Beer, P. D. Indolocarbazoles: A New Family of Anion Sensors. *Chem. Commun.* **2005**, 236−238.
(42) Fatila, E. M.; Twum, E. B.; Sengupta, A.; Pink, M.; Karty, J. A.; Raghavachari, K.; Flood, A. H. Anions Stabilize Each Other inside Macrocyclic Hosts. *Angew. Chem., Int. Ed.* **2016**, *55*, 14057−14062.
(43) Kim, D. W.; Jeong, H.; Lim, S. T.; Sohn, M. Facile Nucleophilic Fluorination of Primary Alkyl Halides Using Tetrabutylammonium Fluoride in A *tert*-Alcohol Medium. *Tetrahedron Lett.* **2010**, *51*, 432−434.
(44) Abbas, I. I.; Hammud, H. H.; Shamsaldeen, H. Calix[4]pyrrole Macrocycle: Extraction of Fluoride Anions from Aqueous Media. *Eur. J. Chem.* **2012**, *3*, 156−162.
(45) Bose, P.; Dutta, R.; Santra, S.; Chowdhury, B.; Ghosh, P. Combined Solution-Phase, Solid-Phase and Phase-Interface Anion Binding and Extraction Studies by a Simple Tripodal Thiourea Receptor. *Eur. J. Inorg. Chem.* **2012**, *2012* (35), 5791−5801.
(46) Aydogan, A.; Coady, D. J.; Lynch, V. M.; Akar, A.; Bielawski, C. W.; Marquez, M.; Sessler, J. L. Poly(methyl methacrylate)s with Pendant Calixpyrroles: Polymeric Extractants for Halide Anion Salts. *Chem. Commun.* **2008**, 1455−1457.
(47) Cardona, C. M.; Gawley, R. E. An Improved Synthesis of a Trifurcated Newkome-Type Monomer and Orthogonally Protected Two-Generation Dendrons. *J. Org. Chem.* **2002**, *67*, 1411−1413.

DOI: 10.1021/acs.joc.9b00042
J. Org. Chem. 2019, 84, 4050−4057